



SWATH-MS as a strategy for CHO host cell protein identification and quantification supporting the characterization of mAb purification platforms

Sofia B. Carvalho^{a,b}, Ludivine Profit^c, Sushmitha Krishnan^d, Ricardo A. Gomes^{a,b}, Bruno M. Alexandre^{a,b}, Severine Clavier^e, Michael Hoffman^d, Kevin Brower^{d,*}, Patrícia Gomes-Alves^{a,b,**}

^a iBET, Instituto de Biologia Experimental e Tecnológica, Apartado 12, Oeiras 2780-901, Portugal

^b ITQB-NOVA, Instituto de Tecnologia Química e Biológica António Xavier, Universidade Nova de Lisboa, Av. Da República, Oeiras 2780-157, Portugal

^c Mammalian Platform, Global CMC Development, Sanofi R&D, Vitry-sur-Seine, France

^d Mammalian Platform, Global CMC Development, Sanofi R&D, Framingham, MA, USA

^e BioAnalytics, Global CMC Development, Sanofi R&D, Vitry-sur-Seine, France

ARTICLE INFO

Keywords:

mAbs
SWATH-MS
CHO HCP identification
high throughput HCP quantification
Purification platform
Bioprocess development

ABSTRACT

Host cell proteins (HCPs) are process-related impurities expressed by the host cells during biotherapeutics' manufacturing, such as monoclonal antibodies (mAbs). Some challenging HCPs evade clearance during the downstream processing and can be co-purified with the molecule of interest, which may impact product stability, efficacy, and safety. Therefore, HCP content is a critical quality attribute to monitor and quantify across the bioprocess.

Here we explored a mass spectrometry (MS)-based proteomics tool, the sequential window acquisition of all theoretical fragment-ion spectra (SWATH) strategy, as an orthogonal method to traditional ELISA. The SWATH workflow was applied for high-throughput individual HCP identification and quantification, supporting characterization of a mAb purification platform. The design space of HCP clearance of two polishing resins was evaluated through a design of experiment study. Absolute quantification of high-risk HCPs was achieved (reaching 1.8 and 4.2 ppm limits of quantification, for HCP A and B respectively) using HCP-specific synthetic heavy labeled peptide calibration curves. Profiling of other HCPs was also possible using an average calibration curve (using labeled peptides from different HCPs). The SWATH approach is a powerful tool for HCP assessment during bioprocess development enabling simultaneous monitoring and quantification of different individual HCPs and improving process understanding of their clearance.

1. Introduction

Host cell proteins (HCPs) are process-related impurities expressed by host cells during the production of biologics, such as monoclonal antibodies (mAbs). Some HCPs are problematic due to their biological enzymatic activity or immunogenicity profile, reducing product efficacy

or posing potential safety risks for patients (Husson et al., 2018; Vanderlaan et al., 2018; Walker et al., 2017). Although most HCPs are effectively eliminated during the purification process, some are more challenging to remove and are commonly present in the drug product (Huang et al., 2021). Therefore, it is critical to monitor residual HCPs during bioprocessing steps (Sim et al., 2020). Current guidelines

Abbreviations: HCPs, Host cell proteins; DSP, downstream processing; MS, mass spectrometry; SWATH, sequential window acquisition of all theoretical fragment-ion spectra; DoE, design of experiment; DDA, Data-dependent acquisition; MRM, multiple reaction monitoring; PRM, parallel reaction monitoring; DIA, data independent acquisition; CBH, Clarified bulk harvest; CHO, Chinese hamster ovary; FT, Protein A Flowthrough; Wash, Protein A wash; PAE, Protein A eluate; AEX, Anion exchange; HIC, Hydrophobic interaction chromatography; Ambic, ammonium bicarbonate; DTT, DL-Dithiothreitol; IAA, Iodoacetamide; TFA, Trifluoroacetic acid.

* Corresponding author.

** Corresponding author at: iBET, Instituto de Biologia Experimental e Tecnológica, Apartado 12, Oeiras 2780-901, Portugal

E-mail addresses: Kevin.Brower@sanofi.com (K. Brower), palves@ibet.pt (P. Gomes-Alves).

<https://doi.org/10.1016/j.jbiotec.2024.02.001>

Received 18 October 2023; Received in revised form 17 January 2024; Accepted 5 February 2024

Available online 8 February 2024

0168-1656/© 2024 The Authors. Published by Elsevier B.V. This is an open access article under the CC BY-NC-ND license (<http://creativecommons.org/licenses/by-nc-nd/4.0/>).

recommend total HCP levels in the final drug substance (DS) to be typically under 100 ppm (Gilgunn and Bones, 2018). The wide dynamic range of concentrations comprising residual HCP levels as well as the highly concentrated product of interest is one of the major challenges of HCP quantification (Vanderlaan et al., 2018).

To the present date, enzyme-linked immunosorbent assay (ELISA) is the gold-standard method for total HCP quantification, mainly due to its robustness, simplicity, and high-throughput capacity (Esser-Skala et al., 2020). However, this method presents several drawbacks: it does not provide HCP identification data and there is no information on the antigens being measured on the commercially available kits; sensitivity depends on the immunogenicity of each HCP during reagent generation, which implies that some HCPs may not be detected even if present; individual HCPs levels may exceed the specific antibody available, meaning that quantification may be underestimated; and the method does not discriminate if the HCP amounts are from an individual HCP or a sum of several HCPs (Husson et al., 2018; Walker et al., 2017).

To improve process understanding it is critical to obtain a comprehensive profiling of HCPs, knowing their identity and their individual levels to evaluate how process conditions impact HCP clearance and to guide process optimization in terms of HCP removal (Gilgunn and Bones, 2018). Advances in the biologics field, emergence of new technologies, and revision of regulatory requirements are pushing the development of improved tools and the use of orthogonal methods to support ELISA data (European Pharmacopoeia. European Pharmacopoeia., 2017; US Pharmacopoeia. Residual host cell protein measurement in biopharmaceuticals. USP 39 Published General Chapter <1132>., 2016; ICH., 2021; ICH Expert Working Group, 1999).

Mass spectrometry (MS)-based methods for HCP identification and quantification are being explored, and recommended by regulatory authorities, as orthogonal and complementary approaches to ELISA assays (European Pharmacopoeia. European Pharmacopoeia., 2017; US Pharmacopoeia., 2016; “USP., 2015–2020. Available from: <https://callforcandidates.usp.org/node/20136>,” n.d.). Data-dependent acquisition (DDA)-based methods have been most commonly used for qualitative proteomics and have been reported as suitable to monitor and analyze HCPs during manufacturing (Sim et al., 2020). In a DDA experiment, there is a limited number of ions that are selected for MS/MS fragmentation. Although high-spectral quality is obtained for the selected peptides, this means that low abundant HCPs may be missed (Pilely et al., 2022). Moreover, the stochastic nature of fragmentation/peptide sampling requires multidimensional separation steps coupled with lengthy chromatographic gradients, which limits throughput and the viability to use these methods for bioprocess development and optimization (Lange et al., 2008; Picotti and Aebersold, 2012; Sim et al., 2020). To address these challenges, targeted approaches were implemented, such as multiple reaction monitoring (MRM) (Carr et al., 2014) or parallel reaction monitoring (PRM) (Bourmaud et al., 2016; Peterson et al., 2012). These approaches deliver high specificity and sensitivity since predetermined pairs of precursor/fragments (i.e., transitions) are measured. However, the number of transitions is limited, even when time-scheduled transitions are used (transitions are only monitored during a specific time window which is set according to their respective retention times). Hence, these methods can only be used when the HCPs to be monitored are previously established. Moreover, the list of critical HCPs is not always known *a priori*, as HCP co-purification is usually dependent on product-specific binding, or interactions with, for example, protein A resin (Jones et al., 2021; Walker et al., 2017). As an alternative, data independent acquisition (DIA) (reviewed in (Zhang et al., 2020)) can be used for the simultaneous quantitation of all HCPs identified, overcoming the limitations of traditional DDA-based methods and eliminating the need for targeted analysis (Gillet et al., 2012; Hessmann et al., 2023; Panchaud et al., 2011; Purvine et al., 2003; Sebastião et al., 2020, 2018, 2019; Silva et al., 2006; Simã Strasser et al., 2021; Trauchessec et al., 2021). Sequential window acquisition of all theoretical fragment-ion spectra

Table 1

List of 9 commonly found HCPs used to generate an average standard calibration curve.

HCP	UniProt ID (CRIGR)
Cathepsin D	G314W7_CRIGR
Serine protease HTRA1	G31BF4_CRIGR
Putative phospholipase B-Like 2	G316T1_CRIGR
Lipoprotein Lipase	G3H6V7_CRIGR
Peroxioredoxin-1	G3GYP9_CRIGR
Phospholipid transfer protein	G3H8V4_CRIGR
Galectin	G314Z7_CRIGR
Ubiquitin	G31129_CRIGR
Clusterin	G3HNJ3_CRIGR

(SWATH) is a DIA-MS approach that performs fragmentation of all precursor ions through a sequential series of specified mass ranges (windows). SWATH relies on targeted data extraction and uses a specific ion spectral library to enable the extraction of high-quality quantitative measurements (Sim et al., 2020; Walker et al., 2017). This method has been reported as suitable for HCP profiling during bioprocess development (Blethrow and Johansen, 1997; Sim et al., 2020; Walker et al., 2017), presenting a high reproducible performance (Collins et al., 2017). However, processing and analyzing the amount of data generated during SWATH analysis is still a challenge, often requiring tailored bioinformatic tools to increase throughput and decrease the number of false positives (Ludwig et al., 2018; Rosenberger et al., 2017).

Here, we implemented a SWATH-MS workflow that enables simultaneous detection and quantification (absolute or semi-absolute, for some HCPs below 1 ppm range) of individual HCPs, including some that were unknown *a priori*. These quantifications rely on specific calibration curves, using specific heavy labeled peptides (synthetic peptides labeled with heavy isotopes) of a target HCP, or on an average calibration curve (using heavy labeled peptides from several HCPs). Nine different HCPs (Table 1) were selected as targets for absolute quantification. These proteins are considered high-risk HCPs being potentially relevant to support the characterization of our platform workflow. As an example, Serine protease is a problematic HCP due to its potential impact on drug quality. This HCP has been reported to degrade mAbs in some cases (Jones et al., 2021).

The SWATH method was applied to evaluate the HCP removal capacity of a mAb purification platform, focusing on two polishing resins, through a Design of Experiment (DoE) methodology. This powerful high throughput tool leverages process understanding and knowledge which is key for bioprocess development and efficient HCP removal. Moreover, it can be used in the scope of regulatory discussions by developing platform understanding of HCP removal across projects, helping to bring high-quality biologics to the market in a faster and safer manner.

2. Materials and methods

2.1. Sample generation

2.1.1. Biological material

Materials were generated using Chinese hamster ovary (CHO) cells. Clarified bulk harvest (CBH) and downstream process intermediates of two mAb molecules were used: mAb1 (IgG4) and mAb2 (IgG1).

2.1.2. Chromatographic experiments

2.1.2.1. Chemicals and reagents. Buffers and solutions were prepared using chemicals of analytical grade (Sigma). Buffers were prepared by mixing acid and conjugate base solutions to reach the desired pH. Conductivity was adjusted by sodium chloride addition.

2.1.2.2. Protein A chromatography. mAbs were purified on protein A chromatography columns (20 cm bed height) on an AKTA pure 25 M

workstation (Cytiva) monitored with Unicorn 7.6 software. Protein detection was performed at 280 nm. The protein A column was equilibrated, loaded with the clarified bulk harvest, and washed. The product was then eluted with 25 mM acetate pH 3.7. Clarified Bulk Harvest (CBH), Protein A Flowthrough (FT), Protein A wash (wash) and Protein A eluate (PAE) were sampled for spectral library generation (see Section 2.5.1). Protein A purification runs were operated under non-optimized conditions (neutral wash buffer) to increase the level/number of HCPs.

2.1.2.3. Characterization of polishing resins. Two polishing resins have been studied: polishing 1 is a mixed-mode AEX (anion exchange) resin and polishing 2 is a HIC (hydrophobic interaction chromatography) resin. Both resins are used in flowthrough mode.

2.1.2.3.1. DoE design. The design space of HCP clearance of the two polishing resins have been characterized using Design of Experiment (DoE). The *Custom Design* tool in JMP15 was used to generate a response surface model to study main effects, pairwise interactions, and quadratic effects, yielding 16 chromatography experiments per mAb and polishing resin. The following primary factors have been studied: load factor (100–300 g/L), load pH (4–7 for mAb1 and 5–8 for mAb2) and load NaCl concentration (0–300 mM).

2.1.2.3.2. Polishing chromatography method. Experiments were carried out on a Freedom EVO 200 (Tecan) using OPUS RoboColumn pre-packed columns (Repligen Corporation) of 0.2 mL column volume and 1 cm bed height. The load material was protein A eluate adjusted at the studied pH and salt concentration. Columns were equilibrated to match the load pH and conductivity before loading the material. At the end of the load, the equilibration buffer was used to recover the product. A residence time of 5 minutes was used throughout the process.

2.1.2.4. Protein concentration and total HCP quantification. The purified samples were quantified (total protein content) by UV-Vis using a Big Lumatic spectrophotometer (Unchained Labs). Total HCP content was determined using Gyrolab disc-based immunoassay with the Gyrolab CHO-HCP E3G Kit on the Gyrolab xP workstation (Gyros Protein Technologies).

2.2. SWATH-MS

2.2.1. Chemicals and reagents

Sample digestion was performed using the following reagents: Water LC-MS grade (Fisher Chemical), ammonium bicarbonate (Ambic) (Sigma), RapiGest Surfactant (SF) (Waters), DL-dithiothreitol (DTT) (Sigma), iodoacetamide (IAA) (Sigma), Sequencing Grade Modified Trypsin (Promega), and trifluoroacetic acid LC-MS grade (TFA) (Fisher Chemical). Formic acid 0.1% solution in water LC-MS grade (Fisher Chemical) and formic acid (FA) 0.1% solution in acetonitrile LC-MS grade (Fisher Chemical) were used for LC-MS runs.

2.2.2. Sample preparation

Protein samples were digested with trypsin before LC-MS analysis. In all samples, protein concentration was adjusted to 0.8 µg/µL using 50 mM Ambic. One hundred µg of protein was incubated with RapiGest SF (0.1%) and DTT (5 mM) for 60 min at 60 °C, while mixing at 500 rpm. The reaction mixture was cooled to room temperature and IAA solution (15 mM) was added and incubated for 30 min at room temperature, while mixing at 500 rpm. Trypsin was added to the reaction (2.5 µg) and incubated for 16 hours at 37 °C. The sample was acidified by adding TFA to a final concentration of 1% and incubated for 45 min at 37 °C, 500 rpm mixing. Precipitated RapiGest SF was removed by centrifugation at 21130 g for 15 min. Digested samples were stored at –80 °C until further analysis.

2.2.3. LC-MS analysis strategy

DDA and DIA SWATH acquisition were performed using a TripleTOF

6600 mass spectrometer coupled to Eksigent NanoLC 400 system (in microLC mode) (SCIEX).

2.2.3.1. Spectral peptide library generation. A spectral peptide ion library was generated for the untargeted SWATH analysis of HCPs and the selection of proteotypic peptides for SWATH absolute quantification of target HCPs. A total of 23 protein samples (CBH, FT, wash and PAE) were acquired in DDA mode (Top 50 MSMS) in duplicate. 7.8 µg of each sample were analyzed by MicroLC with a trap-and-elution configuration using a Micro Trap positive C18 0.3 × 10 mm (Phenomenex) and separation column (ChromXP C18-CL, 3 µm 120 Å, 0.3 × 150 mm, Eksigent). Detailed LC and MS parameters are shown in the [supplementary information \(Suppl. Tables 1 and 2\)](#).

The spectral peptide library was created by combining all DDA raw files into a single ProteinPilot software (v5.0 SCIEX) group file search with the Paragon algorithm a CHO database (UP000001075, 23885 proteins from Swiss-Prot & TrEMBL, download date 03/18/2022) supplemented with the heavy and light chains of the respective mAb was used. Proteins within an FDR <1% (Global FDR from fit) were considered. Shared peptides were set not to be imported. A specific spectral library was built for each mAb product analyzed, with 502 proteins for mAb1 and 1074 proteins for mAb2.

2.2.3.2. Selection of proteotypic peptides. For the absolute quantification of target HCPs using DIA-SWATH-MS, two proteotypic peptides for each individual target HCP were selected using the Skyline software (version 22.2.0.255) ([MacLean et al., 2010](#)). Peptides were selected based on the following criteria: 0 missed cleavages; 8–45 amino acid length; exclude peptides containing Cys, Met, His, RP/KP and NXT/NXS motifs; peptides must be present in the peptide library (built based on DDA runs described in Section 2.5.1). The final list of peptides was ranked by intensity levels observed on the peptide library, and two peptides per HCP were selected for the synthesis of heavy labeled peptides (with stable isotope-labeled C-terminal amino acids). The peptides were purchased from PEPSCAN.

2.2.3.3. DIA-SWATH MS. For the quantitative analysis of HCPs by MS, 7.8 µg of protein digest was analyzed by SWATH-MS acquisition in triplicate runs. Chromatographic conditions were similar to the previously described DDA run. SWATH-MS data were acquired using a set of 64 overlapping variable SWATH windows ([Suppl. Table 3](#)), calculated using the SWATH Variable Window Calculator V1.0 (SCIEX).

Each sample was spiked with 20 fmol of the four heavy peptides standards of the HCPs targeted for absolute quantification. MS signals and retention times of the spiked heavy labeled peptides were used as internal controls to ensure system stability. For the absolute quantification of each targeted HCP, an external calibration curve was generated for every heavy-labeled proteotypic peptide selected. Ten calibration points (ranging from 0.25–50 fmol) were analyzed in mAb1 as matrix.

2.2.4. Data analysis

2.2.4.1. DIA-SWATH untargeted data extraction for relative quantification. Untargeted data processing was performed using a SWATH 2.0 processing plug-in for PeakView 2.2 (Sciex) using the spectral peptide libraries. F Manual inspection was performed for the peptides of the target HCPs to check the quality of the data before data processing, and ions were edited when required. Data were processed considering a maximum of 6 peptides per protein and six transitions for each peptide ([Suppl. Table 4](#)).

The SWATH export files containing the peak area of the HCP peptides were used for the relative quantification which compares the levels of each HCP between different samples without the need for a standard curve. The SWATH export file was further analyzed and filtered using an in-house Python-based tool. This tool gathers critical information (that

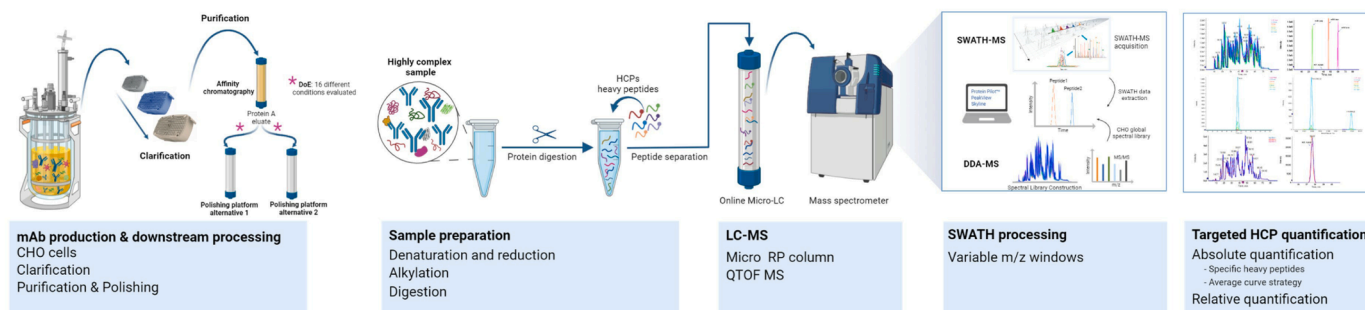


Fig. 1. SWATH-MS approach for HCP landscape characterization. Workflow for sample generation, sample preparation and data acquisition for SWATH-MS based HCP quantification of mAb samples. CHO-derived mAb were clarified and purified by protein A affinity chromatography. A DoE study was performed to characterize two alternative polishing resins using different loading and chromatographic conditions. Digested samples were spiked with heavy peptides specific for targeted HCP and analyzed by SWATH-MS. The SWATH-MS data sets were processed and HCP identification was based on the comprehensive CHO IDA library generated (Suppl. 1). HCP absolute quantification was performed using the heavy peptides to generate calibration curves specific for each HCP or for an average calibration curve (semi-absolute quantification). SWATH data enabled relative quantification of all the HCP identified.

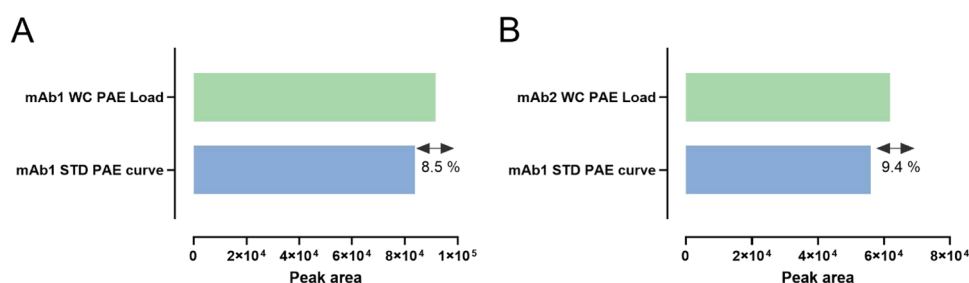


Fig. 2. Matrix effect evaluation. Comparison of a HCP A specific heavy peptide (spiked at 20 fmol) peak area using mAb1 STD PAE or mAb1 WC PAE (protein A eluate purified at worst case scenario conditions) as matrix (C). Comparison of a specific heavy peptide (spiked at 20 fmol) peak area using mAb1 STD PAE or mAb2 WC PAE (protein A eluate purified at worst case scenario conditions) as matrix (D). STD = standard conditions; PAE = Protein A eluate; WC = worst case conditions.

usually is split into different output tables) to guide decisions on considering or discarding any given peptide reported on the export file for quantification purposes. Data was filtered by the removal of true decoys, heavy peptides, proteins quantified by <2 peptides and MS2 spectra with FDR > 0.01 and Score < 1.3.

2.2.4.2. DIA-SWATH targeted data extraction for absolute quantification.

For the absolute quantification of targeted HCPs using SWATH data, the SWATH files were processed using Skyline software (version 22.2.0.255). The default transition settings for proteotypic peptides were used (Suppl. Table 5). Peak integrations were manually checked and curated for each HCP of interest. The correct endogenous peptide was selected based on the heavy peptide signal. Fragment peak areas from the endogenous light peptide and the heavy labeled internal standard were used for the absolute quantification of each target HCP.

The peak areas of these heavy peptides were used to generate external calibration curves for HCP A and HCP B. A log₂ transformation was applied to stabilize data variance of higher concentrations/peak areas. The quantifier peptide and the best transition were selected after the analysis of the calibration curves (i.e., three transitions per peptide and two peptides per HCP). Selection criteria included: CV <20% among technical triplicates, correlation coefficient (R^2) >0.99 and signal intensity. Calibration curves $y=a_0+a_1x$ were obtained using a linear regression model and the coefficient of variation (CV) was calculated for each concentration level. The amount of each endogenous HCP in the samples was determined using the external calibration curves normalized by the corresponding internal standard (IS) (heavy peptide spiked in each sample at 20 fmol). The concentration of each HCP was expressed in ppm taking into consideration the molecular weight of the target HCP.

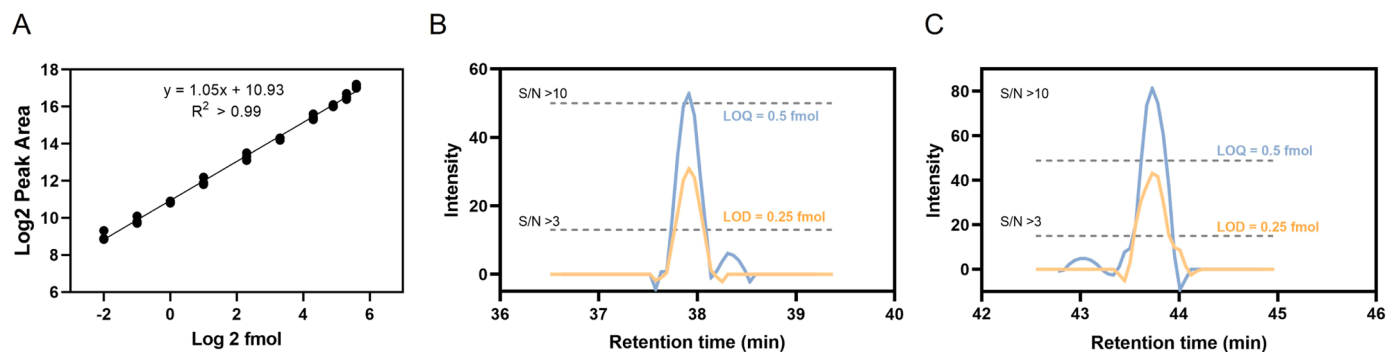


Fig. 3. HCP A calibration curve. LOD and LOQ for HCP A and HCP B. Representative calibration curve of heavy peptide 1 from HCP A. Calibration points ranged from 0.25 to 50 fmol. Peak areas and concentrations were log₂ transformed (A). Limit of detection (LOD) and limit of quantification (LOQ) definition using signal to noise (S/N) approach (LOD corresponds to a concentration where S/N >3 and LOQ corresponds to a concentration where S/N >10) for HCP A (B) and HCP B (C).

2.2.4.3. DIA-SWATH for semi-absolute quantification of non-target HCPs. SWATH-MS data was also used for semi-absolute quantification of any HCPs present in the samples (and previously identified through the ion library). This was achieved using a generic average standard curve with several heavy-labeled peptides from 9 different HCPs (Table 1). Further analysis was performed as described for absolute quantification (see Section 2.6.2).

2.2.4.4. Statistical analysis. All Statistical analyses were performed using GraphPad version 9.1.1 (Dotmatics, San Diego, CA, USA). Differences (%) between the HCP A concentration obtained using individual calibration curve (with specific heavy labeled peptides) and average calibration curve (using heavy labeled peptides from several commonly found HCPs) were assessed using a Bland–Altman analysis (Bland and Altman, 1986). From this analysis, the mean bias indicates the average deviation between the two quantification methods whereas the limit of agreement corresponds to the 95% confidence interval for the differences. The closer to zero the mean bias is, and the smaller the range between the limits of agreement, the more similar are the evaluated results.

2.2.5. Method validation for absolute quantification

Method validation was performed according to the European Medicines Agency (EMA) guidelines on bioanalytical method validation (E.M.A. European Medicines Agency., 2011). Parameters evaluated were matrix effect/specificity, linearity, threshold of detection, threshold of

quantification, precision and accuracy. For more information, please see [Supplementary Information](#).

3. Results and discussion

3.1. SWATH-MS approach for HCP identification and quantification

The SWATH-MS HCP quantification approach reported here was developed following the workflows described in Fig. 1 and Suppl. 1. This method was designed to characterize the HCP clearance capacity of a purification platform developed for mAbs and related molecules (antibody-drug conjugates, multi-specific antibodies, Fc-Fusion proteins, or hybrids). Two polishing resins, with orthogonal modes of interaction, were studied: a mixed-mode AEX resin and a HIC resin, both operated in flowthrough mode. The design space of HCP clearance was evaluated using Design of Experiments (DoE) over a wide range of operating conditions (pH, salt concentration and load factor). HCP profiling and quantification was performed using DIA-SWATH-MS. This method allows for the untargeted HCP identification and relative quantification, using a spectral ion library for data analysis. To enrich the spectral peptide library, protein A purification runs were performed under non-optimized conditions (neutral wash buffer) that increase the level of HCPs. Additionally, the analysis of samples that do not contain the highly abundant mAb peptides (FT and wash), reduces the dynamic range and data noise, increasing the number of HCP identifications. A different library was generated for each specific mAb molecule analyzed

Table 2

Method precision analysis. Intra-assay variability was evaluated by analyzing mAb1 PAE STD sample (with a known concentration of endogenous HCP A) spiked with 8 different concentrations of an HCP A heavy-labeled peptide in triplicate ($n = 24$). The intra-assay variability was determined by calculating the HCP A endogenous concentration and the CV considering all 24 points and only the 3 points corresponding to the 20 fmol spiking (the amount used for samples spiking). Inter-assay variability was assessed by conducting 3 independent runs and measuring HCP A endogenous concentration in 8 mAb1 PAE samples per run (from three independent digestions), spiked with different concentrations of an HCP A heavy-labeled peptide. The inter-assay variability was determined by calculating the average HCP A endogenous concentration and the CV for all the spiking concentrations (highlighted in yellow, bottom row).

Intra-assay variability							
Sample	Spiking (fmol)	n	[HCP A] _{expected} (fmol)	Avg [HCP A] _{measured} (fmol)	stdev (fmol)	CV (%)	
mAb1 PAE STD	1 – 50	24	20	20.8	2.3	11.3	
	20	3		20.2	1.2	5.9	
Inter-assay variability							
Sample	Spiking (fmol)	Run #	n	[HCP A] _{expected} (fmol)	Avg [HCP A] _{measured} (fmol)	stdev (fmol)	CV (%)
mAb1 PAE STD	1	1,2,3	3	20	18.1	0.3	1.5
	2	1,2,3	3		17.1	0.8	4.9
	5	1,2,3	3		19.0	1.7	8.7
	10	1,2,3	3		23.8	2.0	8.4
	20	1,2,3	3		19.4	2.0	10.3
	30	1,2,3	3		21.8	2.3	10.5
	40	1,2,3	3		22.7	2.2	9.6
	50	1,2,3	3		19.2	1.0	5.4
mAb1 PAE STD	1 - 50	1,2,3	3	20	20.0	2.6	12.9

Table 3

Method accuracy was assessed by measuring the recovery of samples at three spiking concentration levels, 1, 20 and 40 fmol. mAb1 matrix PAE sample was spiked with an HCP A heavy-labeled peptide and the recovery was calculated. Accepted recovery ranges were defined based on the EMA guidelines (E.M.A. European Medicines Agency, 2011).

[HCP A] _{spiked} (fmol)	[HCP A] _{measured} (fmol)	Recovery (%)
1	1.2	117.0
1	1.0	103.1
20	18.8	93.8
20	21.0	105.2
40	40.8	101.9
40	42.7	106.8

in this study, which is critical to improve HCP identification and quantification, decreasing the number of false identifications. With the inclusion of heavy labeled peptides specific to targeted HCPs (known *a priori*), absolute quantification was performed using the SWATH-MS data with targeted data extraction (Husson et al., 2018). HCP A and HCP B were defined as target HCPs for absolute quantification. Moreover, the addition of heavy peptides from seven other commonly found and problematic HCPs (2 proteotypic peptides per HCP, 14 peptides in total), were used to generate an average calibration curve (Jones et al., 2021). This enables the semi-absolute quantification of unexpected HCPs identified using the untargeted SWATH-MS analysis.

3.2. SWATH-MS absolute-quantification method validation

The absolute quantification method validation included analysis of matrix effect, linearity, precision and accuracy, threshold of detection and quantification parameters. To investigate the matrix effect, we determined the peak area of a HCP A-specific heavy-labeled peptide using different mAb matrices (mAb1 and mAb2) and purification strategies (STD or WC scenario conditions). Fig. 2A shows that the heavy peptide peak area is similar for different purification conditions. There is a slight difference of 8.5%, higher for the WC purification when compared to the STD. Moreover, using a different mAb molecule the peak area variation is also comparable for both conditions, being 9.4% higher for the mAb2 WC PAE sample (Fig. 2B). This data indicates that the matrix selected for the calibration curve generation (mAb1 PAE STD) is representative of the samples to be analyzed.

For each targeted HCP, two proteotypic peptides were selected according to the criteria described in Section 2.5.2. The peak areas for each transition (MS/MS) of these heavy labeled peptides, at different

concentrations, were determined and used to generate individual calibration curves. The calibration curve of each transition/peptide was evaluated according to the acceptance criteria: CV (triplicate runs per point) < 25% and $R^2 > 0.99$. Peptide transitions that do not meet these criteria were excluded. For each peptide, the quantification reported was based on only one transition (the final selection step of the best transition per peptide was based on signal intensity). The quantification was also verified by a second peptide. Fig. 3A depicts a representative calibration curve for heavy peptide 1 of HCP A ($R^2 > 0.99$). The linear quantification range can be established from 0.25 up to 50 fmol, with all calibration curve points presenting CVs below the 25% threshold. The limit of detection (LOD) and limit of quantification (LOQ) were calculated based on the signal-to-noise ratio (European Medicines Agency, 1995). For HCP A estimation of LOD and LOQ was 0.25 fmol and 0.5 fmol, respectively, corresponding to 2.1 and 4.2 ppm (Fig. 3B). For HCP B, the LOD was set at 0.25 fmol (0.92 ppm) and LOQ at 0.5 fmol (1.84 ppm) (Fig. 3C). These values are within the expected range of HCPs in biologics. It also demonstrates that the method has the sensitivity and the capability to detect and quantify low-range concentrations of HCPs (low ppm range), even with the wide dynamic range of concentrations present. Moreover, as the SWATH method described here intends to provide a high throughput tool for polishing platform characterization and screening of bioprocess purification conditions, this range of operation supports the objective.

Method precision was assessed by measuring the intra and inter-assay variability (Table 2). The mAb1 PAE STD sample was spiked with eight different concentrations (from 1 to 50 fmol) of the HCP A-specific heavy-labeled peptide (n=24, triplicates of injection in the same run). Endogenous HCP A concentration was calculated for each condition. The intra-assay CV results were consistent, presenting values around 11% (for the 24 points) or below 6% (for 20 fmol (n=3), the amount used for samples spiking), revealing good repeatability. Inter-assay variability was assessed by analyzing three independent sample preparations and SWATH runs. Individual CV values for each spiking condition (8 different spiking concentrations evaluated) were between 1.5% and 10.5%. Considering all the spiking concentrations, the average CV value is below 13%, which indicates a good intermediate precision. Moreover, we investigated if samples could be quantified using a calibration curve from an independent SWATH run. Differences observed in a reference sample quantification results obtained with a curve run in the same batch or with a curve previously run (a few weeks before) are within the method variability described (20.8 fmol vs 20.6 fmol, respectively). These results suggest that calibration curves from independent SWATH runs could be considered in future quantification

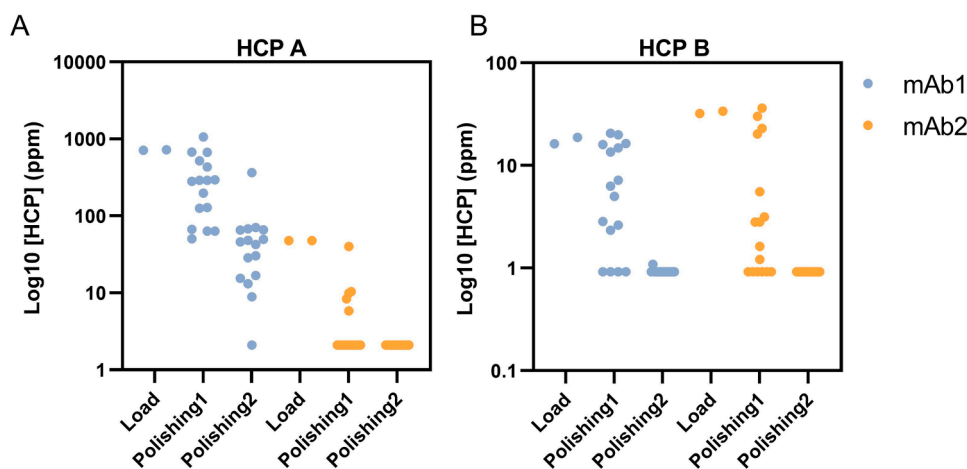


Fig. 4. SWATH-MS HCP absolute quantification. HCP A (A) and HCP B (B) absolute quantification for the load and the 16 different DoE conditions evaluated for polishing resin 1 and polishing resin 2 for both mAb1 (blue circle marker) and mAb2 (orange circle marker) molecules. The LOQ values are plotted for the conditions where the levels of HCP are below this threshold.

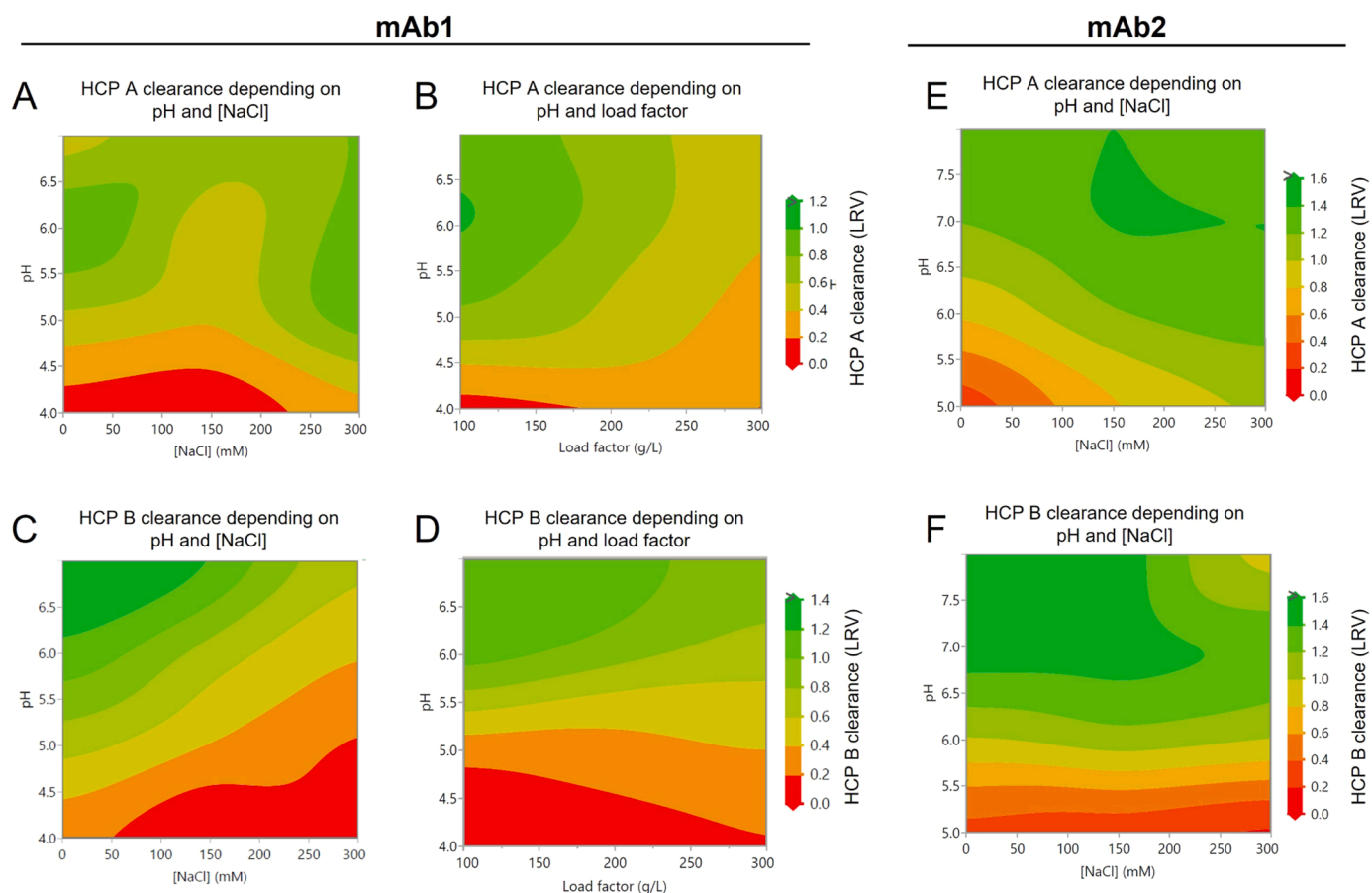


Fig. 5. Design space of HCP A and HCP B clearance by polishing 1 resin for mAb1 and mAb2. The contour plots were obtained from SWATH-MS HCP absolute quantification data using a Design Of Experiment (DoE) including pH, NaCl concentration and load factor parameters. Only parameters with a statically significant impact ($p < 0.05$) are plotted. For samples where the HCP was not detected, the LOD was used to calculate the Log Reduction Value (LRV).

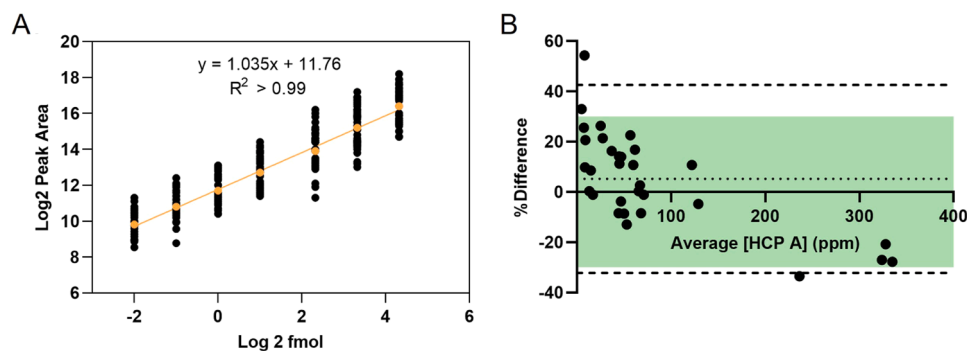


Fig. 6. Average calibration curve. Representative average calibration curve containing 13 different heavy peptides from 9 different HCPs. Linear regression was performed using the average values (orange markers) (A). Bland-Altman plot representing the difference (%) between HCP A concentration calculated using specific or average calibration curves (average between both methods). The dashed lines represent the limits of agreement given by the 95% confidence intervals for the mean bias and the dotted line represents the mean bias from the Bland-Altman plot (the closest to zero, the more similar the results evaluated). The green area covers the 30% acceptable variation for the SWATH method. (B).

studies. Method accuracy was assessed over three spiking concentration levels by calculating the recovery (ratio between the concentration calculated based on the calibration curve and the theoretical concentration of each spiked sample). Table 3 shows that the recovery values are within the regulatory established ranges. These results confirm the suitability of the DIA-SWATH method for the absolute quantification of HCP A.

3.3. Targeted HCP absolute quantification for polishing platform characterization

After implementing the SWATH-MS method for absolute quantification, HCP A and HCP B were targeted as model HCPs to characterize the design space of clearance for two polishing resins (polishing 1, AEX and polishing 2, HIC) for two distinct mAb molecules (mAb1 and mAb2). The load samples (Protein A eluates) and the 16 DoE conditions per resin were analyzed for HCP absolute quantification (Fig. 4). Focusing on HCP

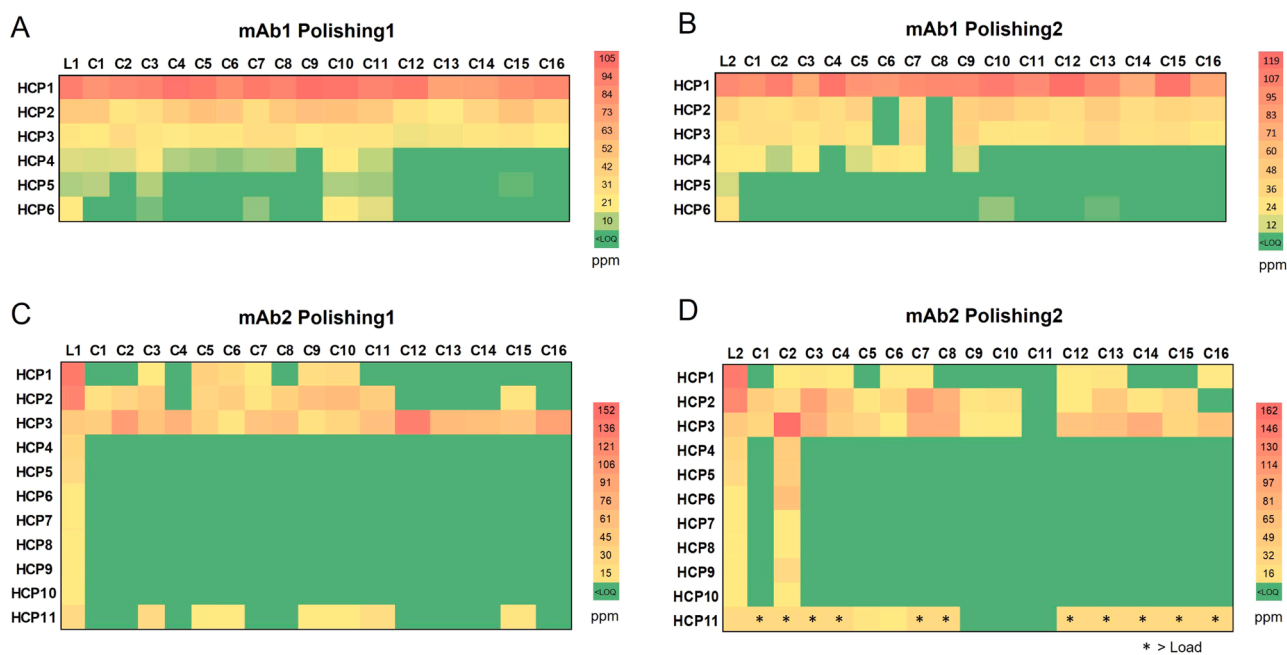


Fig. 7. HCP landscape characterization. Semi-absolute quantification of untargeted HCPs identified after filtering and manual curation of SWATH–MS data. Analysis for mAb1, polishing resin 1 (A) and polishing resin 2 (B) and for mAb2, polishing resin 1 (C) and polishing resin 2 (D). L =loading, C= DoE condition. HCP concentration is presented according to the color scale. HCP identification list is reported in Suppl. Table 8. Conditions that presented values above the load are highlighted with *.

A (Fig. 4A), the starting level in the Load samples of mAb1 is drastically higher when compared to mAb2 (716 ppm vs 48 ppm). However, we observed the same trends between the 2 mAbs in terms of clearance by the polishing resins. HCP A removal is dependent on the operating conditions evaluated for polishing 1 resin, presenting concentration values widely distributed, whereas polishing 2 resin robustly clears this HCP for all tested conditions. For mAb1, one of the conditions presents a HCP A level higher than the Load (1060 ppm). This unexpected result may be related to the aggregation of the mAb molecule observed for this condition (low pH and high salt concentration) potentially causing some interference with the MS signal. The quantification of HCP B (Fig. 4B) presented a range of absolute values much lower compared to HCP A. For the two mAbs, polishing 2 resin showed again a superior removal capacity with almost all conditions being able to remove the HCP (only one condition presenting a concentration of 1 ppm) compared to polishing 1 resin.

Since polishing 2 resin showed robust clearance over a wide range of process parameters, a focus on polishing 1 resin was made for the DoE analysis. Fig. 5 shows the contour plots of HCP A and HCP B clearance obtained from the DoE model, for both molecules. Results are expressed in Log Reduction Value (LRV), defined as the logarithm of the ratio of the absolute levels of HCP in the Load sample and the polishing sample. Overall, the clearance of both HCPs is strongly impacted by pH, with best performances obtained at higher pH. The mode of separation of polishing 1 resin is mainly based on electrostatic interactions. High pH is expected to favor the interactions between the HCP and the positively charged ligand, by reducing the net charge of the HCP (theoretical pI (isoelectric point) of both HCPs is above 5.5) (Jones et al., 2021). The impact of NaCl addition depends on the HCP. For HCP B (Fig. 5C and 5F), clearance decreases with NaCl concentration at high pH. Increasing the ionic strength induces competition, weakening the interaction between the ligand and the HCP, which begins to elute. However, for HCP A, better clearance performance is observed for conditions with increasing NaCl concentration (Fig. 5A and 5E). In this case, salt addition could enable salting-out effects participating to the interaction between the hydrophobic moieties of both the ligand and the HCP, especially when nearing the isoelectric point of the protein. Potential

disruption of local repulsive charges may also favor the retention of this HCP under high salts conditions. Finally, the impact of the load factor was significant only for mAb1. For both HCPs, the clearance decreases with the load factor at high pH, when ligand availability becomes potentially limiting, leading to a gradual breakthrough of the HCP (Figs. 5B and 5D).

These results highlight the different behavior and selectivity of the resins against specific HCPs, emphasizing the complementarity of total HCP quantification vs individual HCP identification. It reinforces the need to have several purification steps with orthogonal interaction in a platform process. The various HCPs produced during the cell culture will exhibit different molecular properties such as charge, hydrophobicity, size, and will interact specifically with each resin. Furthermore, characterizing the behavior of HCPs individually against a wide range of conditions, for each platform resin, allows to further design and optimize new purification processes by selecting the proper resin and conditions to remove a specific contaminant.

3.4. HCP landscape characterization

One main advantage of DIA-SWATH MS method over the targeted MRM-MS method for absolute quantification is that it enables the unbiased non-targeted detection of HCPs using the ion library generated. Using this approach, we identified 6 additional HCP for mAb1 and 11 additional HCPs for mAb2 (i.e., HCPs not targeted and therefore without heavy labeled peptides). To perform a semi-absolute quantification of identified untargeted HCPs, we evaluated the use of an average calibration curve using the peak areas of all the spiked heavy peptides (from different commonly found HCPs) (Fig. 6A). We hypothesized that, although the MS response intensity varies according to the peptide sequence, an average calibration curve with a large population of peptides would balance out the peptides' specific MS detection signal. A generic/"universal" calibration curve could be suitable for the quantification of any HCP in the samples under study, considering the risk of being more accurate for some proteins than for others, depending on the peptides used. To evaluate the suitability of the semi-absolute quantification approach, we compared the quantification of HCP A using its

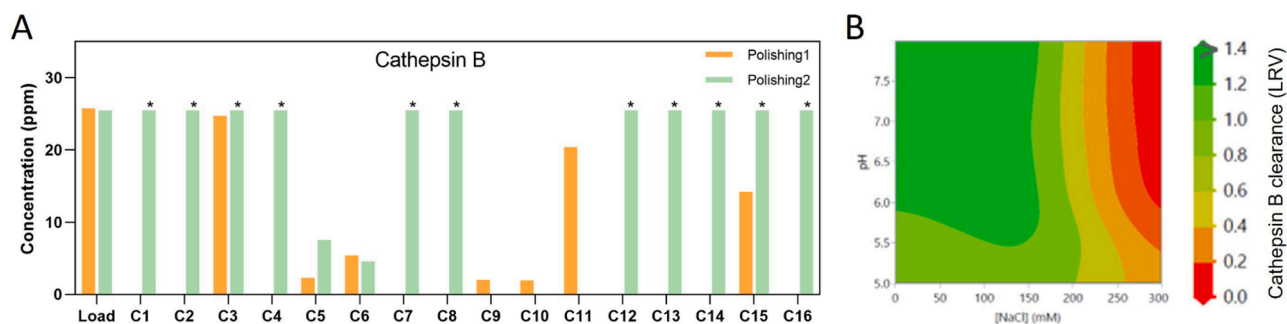


Fig. 8. Quantification of Cathepsin B. Semi-absolute quantification of Cathepsin B HCP calculated using the average calibration curve. Load and DoE conditions values are represented for polishing resin 1 (orange bars) and polishing resin 2 (green bars). (C). Design space of Cathepsin B clearance for mAb2 and polishing 2 resin obtained from the DoE model (D). Conditions that presented values above the load are highlighted with *.

individual calibration curve with specific heavy labeled peptides and using the average curve, for both mAb1 and mAb2 samples. HCP A quantification is comparable for both methods, as indicated by the Bland-Altman plot (Fig. 6B). The mean bias is small (5.2%) and most of the differences are within the limits of agreement (from -32.2% to 42.5%). A difference of 30% was used as an acceptable threshold, analogous to established MS-based quantification methods (Piehowski et al., 2013). The green area depicted in the figure covers this 30% acceptable variation. As observed, except for three conditions, all the measurements are within this range, suggesting that the average curve is suitable for HCP quantification. This strategy represents a great advantage since it allows a semi-absolute quantification of all HCPs detected on the SWATH analysis without having their specific heavy peptides to perform quantification. Similar approaches using standard proteins (not related to the sample) spiked at defined concentrations in the sample preparation step were previously reported (Pilely et al., 2022).

The identified HCPs by the untargeted SWATH-MS analysis were semi-absolutely quantified using the average calibration curve exemplified in Fig. 6A. The Load sample of both mAb molecules and the 16 different conditions for each polishing resin were analyzed (Fig. 7). The concentration of these HCPs is represented according to a color scale code, where green corresponds to 0 ppm ($< \text{LOQ}$) and red to the maximum value observed for each molecule and resin. mAb1 samples present a smaller number of identifications (6 HCPs) and, in general, lower concentration levels when compared to mAb2. This trend is in line with what we observed when analyzing these samples for total HCP content. Comparison of mAb1 total HCP values (measured by ELISA) and absolute quantification of the targeted HCPs (measured by SWATH-MS) showed very similar profiles among the different conditions (Suppl. Table 6). For mAb2 the profiles of both methods are not similar, and the total HCP values are higher than the absolute quantification of the selected HCP (Suppl. Table 7). These results suggest that other undetected HCP(s) may be present in mAb2 samples, contributing to these discrepancies in the profiles. The list of HCPs present in mAb1 samples, and respective removal trends for the different polishing conditions, are similar for both resins (Fig. 7A and Fig. 7B). We can observe that HCP1, HCP2, and HCP3 are identified across almost all the operating conditions tested in the DoE. Particularly, the two polishing resins are inefficient in clearing HCP 1 over the tested operating ranges. This result highlights that other methods of removal, such as protein A wash, should be evaluated for this specific HCP. In the context of this study, high level of HCP1 in the Load might result from the Protein A neutral wash condition. By contrast, HCPs 4–6 are only present in the Load or at low concentrations (< 24 ppm) in the polishing samples. For mAb2, HCPs 1–3 are also the most challenging ones. For both resins, clearance performances vary depending on operating conditions (Fig. 7C and Fig. 7D). Most of the HCPs identified are commonly found in mAb processes using CHO and are not reported as critical.

However, it is interesting to highlight that HCP 11 is Cathepsin B, which is a well-known higher-risk HCP that may impact drug product quality by fragmentation (Jones et al., 2021). The quantification of this HCP was challenging, in particular for polishing resin 2, with several conditions presenting values above the Load (highlighted with *) (Fig. 7D). These values are not in line with what was expected, as we should not observe an enrichment of this HCP. Given this, results suggest that some conditions of polishing resin 2 may be impacting the MS signal, overestimating Cathepsin B quantification. Nevertheless, we are able to assess which conditions are optimal for this HCP clearance (at least in polishing resin 1). Fig. 8A illustrates the concentration values of Cathepsin B for the different conditions of polishing 1 and polishing 2 resins. Cathepsin B level for polishing 1 resin depends on operating conditions ranging from 0 to 25 ppm. Fig. 8B shows the contour plot of Cathepsin B clearance by polishing 1 resin obtained from the DOE model. Clearance is mainly impacted by NaCl concentration. The best result is obtained at pH above 6 (theoretical pI of Cathepsin B is 5.7 based on the sequence (Jones et al., 2021)) and NaCl concentration below 150 mM. Higher NaCl concentration is likely to weaken or even disrupt electrostatic interactions between the HCP and the ligand.

Finally, SWATH data enables a complete HCP landscape characterization, not only identifying all the HCPs present in the sample (and previously identified in the library) but also enabling their relative quantification or semi-absolute quantification (using the average calibration curve). Moreover, this HCP profiling enables also the identification of which ones are “breaking through” the platform polishing resins.

4. Conclusions

The HCP profiles of a biopharmaceutical in both its intermediate and final forms are critical and must be well understood throughout process development. Some HCPs have been identified as high risk due to potential immunogenicity, biological activity, or enzymatic activity with the risk to degrade either product molecules or excipients used in the formulation. The SWATH-MS method described here proved to be suitable for a fast and accurate overview of a CHO HCP landscape in the context of mAb bioprocessing. This approach allows the identification and quantification of individual proteins present in the downstream intermediates.

Using this SWATH-MS tool, with a single experiment, we can assess: 1) absolute quantification of targeted HCPs using calibration curves with specific heavy peptides; 2) relative quantification of all the HCPs identified (if present in a library previously generated); and 3) semi-absolute quantification of untargeted HCPs, taking advantage of an average calibration curve (created with heavy peptides from several commonly found HCPs). Moreover, with SWATH-DIA approach, if new HCPs are identified later, the previously generated library can be updated by adding new proteins to the list, and the acquired sample file can then be

reanalyzed bioinformatically. The developed method is proficient in HCP profiling, at different DSP steps and process conditions, across the wide dynamic ranges observed (mAb vs HCPs).

HCP identification and respective clearance profiles enabled a deeper characterization of a mAb purification platform. This study generated platform knowledge and process understanding on two polishing resins, which is key in guiding bioprocess development. In addition to supporting the characterization of a purification platform, the results also show how one might leverage such analysis when performing process development for a specific therapeutic antibody. The SWATH-MS approach has the potential to become a powerful tool in HCP analysis, assisting high-throughput monitoring, assessing eventual process failures, or evaluating the impact of process changes.

Funding

This work was supported by Sanofi.

CRedit authorship contribution statement

Carvalho Sofia B.: Conceptualization, Formal analysis, Investigation, Methodology, Visualization, Writing – original draft. **Profit Ludivine:** Conceptualization, Formal analysis, Investigation, Visualization, Writing – original draft. **Krishnan Sushmitha:** Conceptualization, Formal analysis, Investigation, Visualization, Writing – original draft. **Gomes Ricardo A.:** Formal analysis, Investigation, Methodology, Writing – review & editing. **Alexandre Bruno M.:** Formal analysis, Investigation, Methodology, Writing – review & editing. **Clavier Severine:** Conceptualization. **Hoffman Michael:** Project administration. **Brower Kevin:** Conceptualization, Funding acquisition, Project administration, Resources, Supervision, Writing – review & editing. **Gomes-Alves Patricia:** Conceptualization, Funding acquisition, Project administration, Resources, Supervision, Writing – review & editing.

Declaration of Competing Interest

The authors declare that they have no known competing financial interests or personal relationships that could have appeared to influence the work reported in this paper.

Data availability

Method implementation key data are in the manuscript and Supporting files. Sanofi's antibody sequence and some chromatographic process details are confidential information and cannot be shared.

Acknowledgements

Authors acknowledge the support from the UniMS team, all MS data were generated by the UniMS–Mass Spectrometry Unit, iBET/ITQB, Oeiras, Portugal. The authors also acknowledge Miguel Antunes and Inês Isidro from iBET Data Science team for their contribution to data analysis. The authors acknowledge the experimental work from Emmanuel Fofie, Céline Hemet and Didier Duthé from Sanofi on chromatographic runs. The authors are grateful to Jason Walther for revising the manuscript and English proofreading.

Data Statement

Method implementation relevant data are in the manuscript and Supporting files. Data containing antibody sequence and some chromatographic process conditions (owned by Sanofi) are confidential information and cannot be shared publicly.

Appendix A. Supporting information

Supplementary data associated with this article can be found in the online version at [doi:10.1016/j.jbiotec.2024.02.001](https://doi.org/10.1016/j.jbiotec.2024.02.001).

References

- Bland, J., Altman, D., 1986. Statistical methods for assessing agreement between two methods of clinical measurement. *Lancet* 327, 307–310. [https://doi.org/10.1016/S0140-6736\(86\)90837-8](https://doi.org/10.1016/S0140-6736(86)90837-8).
- Blethrow, J., Johansen, E., 1997. High Sensitivity Host Protein Quantitation in an IgG1 Monoclonal Antibody Preparation via Data-Independent Acquisition. SCIE X Document number: RUO-MKT-02-6986-B.
- Bourmaud, A., Gallien, S., Domon, B., 2016. Parallel reaction monitoring using quadrupole-Orbitrap mass spectrometer: Principle and applications. *Proteomics* 16, 2146–2159. <https://doi.org/10.1002/pmic.201500543>.
- Carr, S.A., Abbatiello, S.E., Ackermann, B.L., Borchers, C., Domon, B., Deutsch, E.W., Grant, R.P., Hoofnagle, A.N., Hüttenhain, R., Koomen, J.M., Liebler, D.C., Liu, T., MacLean, B., Mani, D., Mansfield, E., Neubert, H., Paulovich, A.G., Reiter, L., Vitek, O., Aebersold, R., Anderson, L., Bethem, R., Blonder, J., Boja, E., Botelho, J., Boyne, M., Bradshaw, R.A., Burlingame, A.L., Chan, D., Keshishian, H., Kuhn, E., Kinsinger, C., Lee, J.S.H., Lee, S.-W., Moritz, R., Oses-Prieto, J., Rifai, N., Ritchie, J., Rodriguez, H., Srinivas, P.R., Townsend, R.R., Van Eyk, J., Whiteley, G., Wiita, A., Weintraub, S., 2014. Targeted peptide measurements in biology and medicine: best practices for mass spectrometry-based assay development using a fit-for-purpose approach. *Mol. Cell. Proteom.* 13, 907–917. <https://doi.org/10.1074/mcp.M113.036095>.
- Collins, B.C., Hunter, C.L., Liu, Y., Schilling, B., Rosenberger, G., Bader, S.L., Chan, D.W., Gibson, B.W., Gingras, A.-C., Held, J.M., Hirayama-Kurogi, M., Hou, G., Krisp, C., Larsen, B., Lin, L., Liu, S., Molloy, M.P., Moritz, R.L., Ohtsuki, S., Schlapbach, R., Selevsek, N., Thomas, S.N., Tzeng, S.-C., Zhang, H., Aebersold, R., 2017. Multi-laboratory assessment of reproducibility, qualitative and quantitative performance of SWATH-mass spectrometry. *Nat. Commun.* 8, 291. <https://doi.org/10.1038/s41467-017-00249-5>.
- E.M.A. European Medicines Agency, 2011. Guideline on Bioanalytical Method Validation In: E.M. Agency (Ed.), London, United Kingdom.
- Esser-Skala, W., Segl, M., Wohlschlager, T., Reisinger, V., Holzmann, J., Huber, C.G., 2020. Exploring sample preparation and data evaluation strategies for enhanced identification of host cell proteins in drug products of therapeutic antibodies and Fc-fusion proteins. *Anal. Bioanal. Chem.* 412, 6583–6593. <https://doi.org/10.1007/s00216-020-02796-1>.
- European Medicines Agency, 1995. ICH Topic Q 2 (R1) Validation of Analytical Procedures: Text and Methodology (CPMP/ICH/381/95).
- European Pharmacopoeia, 2017. *European Pharmacopoeia Monograph 2.6.34. Host-cell protein assays*.
- Gilgunn, S., Bones, J., 2018. Challenges to industrial mAb bioprocessing—removal of host cell proteins in CHO cell bioprocesses. *Curr. Opin. Chem. Eng.* 22, 98–106. <https://doi.org/10.1016/j.coche.2018.08.001>.
- Gillet, L.C., Navarro, P., Tate, S., Röst, H., Selevsek, N., Reiter, L., Bonner, R., Aebersold, R., 2012. Targeted data extraction of the MS/MS spectra generated by data-independent acquisition: a new concept for consistent and accurate proteome analysis. *Mol. Cell. Proteom.* 11, O111.016717 <https://doi.org/10.1074/mcp.O111.016717>.
- Hessmann, S., Chery, C., Sikora, A.-S., Gervais, A., Carapito, C., 2023. Host cell protein quantification workflow using optimized standards combined with data-independent acquisition mass spectrometry. *J. Pharm. Anal.* 13, 494–502. <https://doi.org/10.1016/j.jpba.2023.03.009>.
- Huang, Y., Molden, R., Hu, M., Qiu, H., Li, N., 2021. Toward unbiased identification and comparative quantification of host cell protein impurities by automated iterative LC-MS/MS (HCP-AIMS) for therapeutic protein development. *J. Pharm. Biomed. Anal.* 200, 114069 <https://doi.org/10.1016/j.jpba.2021.114069>.
- Husson, G., Delangle, A., O'Hara, J., Cianferani, S., Gervais, A., Van Dorsselaer, A., Bracewell, D., Carapito, C., 2018. Dual data-independent acquisition approach combining global HCP profiling and absolute quantification of key impurities during bioprocess development. *Anal. Chem.* 90, 1241–1247. <https://doi.org/10.1021/acs.analchem.7b03965>.
- ICH, harmonisation for better health, 2021. ICH Press Release, Continued ICH Growth and Advancement.
- ICH Expert Working Group, 1999. ICH harmonised tripartite guideline specifications: test procedures and acceptance criteria for biotechnological/biological products Q6B.
- Jones, M., Palackal, N., Wang, F., Gaza-Bulsecu, G., Hurkmans, K., Zhao, Y., Chitikila, C., Clavier, S., Liu, S., Menesale, E., Schonenbach, N.S., Sharma, S., Valax, P., Waerner, T., Zhang, L., Connolly, T., 2021. “High-risk” host cell proteins (HCPs): a multi-company collaborative view. *Biotechnol. Bioeng.* 118, 2870–2885. <https://doi.org/10.1002/bit.27808>.
- Lange, V., Picotti, P., Domon, B., Aebersold, R., 2008. Selected reaction monitoring for quantitative proteomics: a tutorial. *Mol. Syst. Biol.* 4, 222. <https://doi.org/10.1038/msb.2008.61>.
- Ludwig, C., Gillet, L., Rosenberger, G., Amon, S., Collins, B.C., Aebersold, R., 2018. Data-independent acquisition-based SWATH - MS for quantitative proteomics: a tutorial. *Mol. Syst. Biol.* 14 <https://doi.org/10.15252/msb.20178126>.
- MacLean, B., Tomazela, D.M., Shulman, N., Chambers, M., Finney, G.L., Frewen, B., Kern, R., Tabb, D.L., Liebler, D.C., MacCoss, M.J., 2010. Skyline: an open source

- document editor for creating and analyzing targeted proteomics experiments. *Bioinformatics* 26, 966–968. <https://doi.org/10.1093/bioinformatics/btq054>.
- Panchaud, A., Jung, S., Shaffer, S.A., Aitchison, J.D., Goodlett, D.R., 2011. Faster, quantitative, and accurate precursor acquisition independent from ion count. *Anal. Chem.* 83, 2250–2257. <https://doi.org/10.1021/ac103079q>.
- Peterson, A.C., Russell, J.D., Bailey, D.J., Westphall, M.S., Coon, J.J., 2012. Parallel reaction monitoring for high resolution and high mass accuracy quantitative, targeted proteomics. *Mol. Cell. Proteom.* 11, 1475–1488. <https://doi.org/10.1074/mcp.O112.020131>.
- Picotti, P., Aebersold, R., 2012. Selected reaction monitoring-based proteomics: workflows, potential, pitfalls and future directions. *Nat. Methods* 9, 555–566. <https://doi.org/10.1038/nmeth.2015>.
- Piehowski, P.D., Petyuk, V.A., Orton, D.J., Xie, F., Moore, R.J., Ramirez-Restrepo, M., Engel, A., Lieberman, A.P., Albin, R.L., Camp, D.G., Smith, R.D., Myers, A.J., 2013. Sources of technical variability in quantitative LC-MS proteomics: human brain tissue sample analysis. *J. Proteome Res.* 12, 2128–2137. <https://doi.org/10.1021/pr301146m>.
- Pilely, K., Johansen, M.R., Lund, R.R., Kofoed, T., Jørgensen, T.K., Skriver, L., Mørtz, E., 2022. Monitoring process-related impurities in biologics—host cell protein analysis. *Anal. Bioanal. Chem.* 414, 747–758. <https://doi.org/10.1007/s00216-021-03648-2>.
- Purvine, S., Eppel*, J.-T., Yi, E.C., Goodlett, D.R., 2003. Shotgun collision-induced dissociation of peptides using a time of flight mass analyzer. *Proteomics* 3, 847–850. <https://doi.org/10.1002/pmic.200300362>.
- Rosenberger, G., Bludau, I., Schmitt, U., Heusel, M., Hunter, C.L., Liu, Y., MacCoss, M.J., MacLean, B.X., Nesvizhskii, A.I., Pedrioli, P.G.A., Reiter, L., Röst, H.L., Tate, S., Ting, Y.S., Collins, B.C., Aebersold, R., 2017. Statistical control of peptide and protein error rates in large-scale targeted data-independent acquisition analyses. *Nat. Methods* 14, 921–927. <https://doi.org/10.1038/nmeth.4398>.
- Sebastião, M.J., Gomes-Alves, P., Reis, I., Sanchez, B., Palacios, I., Serra, M., Alves, P.M., 2020. Bioreactor-based 3D human myocardial ischemia/reperfusion in vitro model: a novel tool to unveil key paracrine factors upon acute myocardial infarction. *Transl. Res.* 215, 57–74. <https://doi.org/10.1016/j.trsl.2019.09.001>.
- Sebastião, M.J., Serra, M., Pereira, R., Palacios, I., Gomes-Alves, P., Alves, P.M., 2019. Human cardiac progenitor cell activation and regeneration mechanisms: exploring a novel myocardial ischemia/reperfusion in vitro model. *Stem Cell Res Ther.* 10, 77. <https://doi.org/10.1186/s13287-019-1174-4>.
- Silva, J.C., Gorenstein, M.V., Li, G.-Z., Vissers, J.P.C., Geromanos, S.J., 2006. Absolute quantification of proteins by LCMSE. *Mol. Cell. Proteom.* 5, 144–156. <https://doi.org/10.1074/mcp.M500230-MCP200>.
- Sim, K.H., Liu, L.C.-Y., Tan, H.T., Tan, K., Ng, D., Zhang, W., Yang, Y., Tate, S., Bi, X., 2020. A comprehensive CHO SWATH-MS spectral library for robust quantitative profiling of 10,000 proteins. *Sci. Data* 7, 263. <https://doi.org/10.1038/s41597-020-00594-z>.
- Simão, D., Silva, M.M., Terrasso, A.P., Arez, F., Sousa, M.F.Q., Mehrjardi, N.Z., Šarić, T., Gomes-Alves, P., Raimundo, N., Alves, P.M., Brito, C., 2018. Recapitulation of human neural microenvironment signatures in iPSC-derived NPC 3D differentiation. *Stem Cell Rep.* 11, 552–564. <https://doi.org/10.1016/j.stemcr.2018.06.020>.
- Strasser, L., Oliviero, G., Jakes, C., Zaborowska, I., Floris, P., Ribeiro da Silva, M., Füssl, F., Carillo, S., Bones, J., 2021. Detection and quantitation of host cell proteins in monoclonal antibody drug products using automated sample preparation and data-independent acquisition LC-MS/MS. *J. Pharm. Anal.* 11, 726–731. <https://doi.org/10.1016/j.jpha.2021.05.002>.
- Trauchessec, M., Hesse, A.M., Kraut, A., Berard, Y., Herment, L., Fortin, T., Bruley, C., Ferro, M., Manin, C., 2021. An innovative standard for LC-MS-based HCP profiling and accurate quantity assessment: Application to batch consistency in viral vaccine samples. *Proteomics* 21. <https://doi.org/10.1002/pmic.202000152>.
- U.S. Pharmacopeia. Residual host cell protein measurement in biopharmaceuticals. USP 39 Published General Chapter <1132>., 2016.
- USP. Call for candidates: host cell protein standards 2015-2020. Available from: <https://callforcandidates.usp.org/node/20136> [WWW Document], n.d.
- Vanderlaan, M., Zhu-Shimoni, J., Lin, S., Gunawan, F., Waerner, T., Van Cott, K.E., 2018. Experience with host cell protein impurities in biopharmaceuticals. *Biotechnol. Prog.* 34, 828–837. <https://doi.org/10.1002/btpr.2640>.
- Walker, D.E., Yang, F., Carver, J., Joe, K., Michels, D.A., Yu, X.C., 2017. A modular and adaptive mass spectrometry-based platform for support of bioprocess development toward optimal host cell protein clearance. *MABs* 9, 654–663. <https://doi.org/10.1080/19420862.2017.1303023>.
- Zhang, F., Ge, W., Ruan, G., Cai, X., Guo, T., 2020. Data-independent acquisition mass spectrometry-based proteomics and software tools: a glimpse in 2020. *Proteomics* 20. <https://doi.org/10.1002/pmic.201900276>.